Plant Soil (2019) 438:223–237
https://doi.org/10.1007/s11104-019-04019-8

REGULAR ARTICLE

Two endophytic bacterial strains modulate Mn oxidation and accumulation in the wetland plant *Suaeda salsa* pall

Guoyan Zhao · Junhui Cheng · Ningning Sun · Changle Ma · Meixue Dai

Received: 17 July 2018 / Accepted: 28 February 2019 / Published online: 9 March 2019

Abstract

Aims Wetlands play vital roles as sinks for metal contaminants. Some wetland plants accumulate manganese (Mn) oxides in the black biofilm around roots and rhizomes, although the underlying mechanism is still unclear. Our aim is to determine the role of endophytic bacteria in the formation of Mn deposits in the wetland plant *Suaeda salsa* Pall. as well as the underlying chemical and molecular mechanisms.

Methods Manganese-oxidizing endophytic bacteria were isolated with leucoberbeline blue (LBB) and further identified via the phylogenetic analysis. The Mn content and black deposit characteristics of laboratory-cultivated plants before/after co-cultivation of bacteria were investigated by inductively-coupled plasma optical emission spectrometry (ICP-OES), a scanning electron microscope equipped with an energy energy-dispersive X-ray spectroscopye (SEM-EDX), and X-ray fluorescence (XRF). The chemical structures of the biogenic Mn minerals were characterized via spectra of X-ray diffraction (XRD), energy-dispersive X-ray spectroscopy (EDX), and selected area electron diffraction (SAED). Proteomic analyses, coupled with the enzymic assays were performed to identify the enzymes involved in the Mn oxidation.

Results We observed black deposits containing Mn oxides in the belowground and aboveground tissues of *S. salsa*. Three Mn-tolerant bacterial strains were isolated from the plants, and two of them possessed Mn(II) oxidation capacities, which were identified as *Pantoea eucrina* SS01 and *Pseudomonas composti* SS02. Co-cultivation of the two isolates with *S. salsa* showed promoted plant growth and facilitated the formation of black precipitations on roots. Further results showed the different chemical compositions and cellular localizations of biogenic Mn oxides from the two strains. Hydrogen peroxide-detoxifying enzymes were involved in Mn oxidation, most likely mitigating oxidative stresses.

Conclusions We suggest a role of endophytic bacteria in Mn uptake and accumulation in the wetland plant *S. salsa*; our study thereby contributes to a better understanding of the plant-endophyte symbiosis in biogeochemical Mn cycling and wetland soil phytoremediation.

Highlights
- Two endophytic Mn-oxidizing bacterial strains promote Mn accumulation in *Suaeda salsa*.
- Diverse Mn oxides are produced by these endophytic bacterial strains.
- Mn oxidation is catalyzed by hydrogen peroxide-detoxifying enzymes.

Guoyan Zhao and Junhui Cheng contributed equally to this work.

Responsible Editor: Juan Barcelo.

Electronic supplementary material The online version of this article (https://doi.org/10.1007/s11104-019-04019-8) contains supplementary material, which is available to authorized users.

G. Zhao (✉) · J. Cheng · N. Sun · C. Ma · M. Dai
College of Life Science, Shandong Normal University, Jinan 250014, People's Republic of China
e-mail: zhaoguoyan@sdnu.edu.cn

G. Zhao · J. Cheng · N. Sun · C. Ma · M. Dai
Shandong Provincial Key Laboratory of Plant Stress Research, Jinan 250014, People's Republic of China

Keywords Phytoremediation · Manganese · Microbial community · Mn-oxidizing bacteria · Oxidative stresses

Abbreviations

ABTS	2,2-azinobis-(3-ethylbenzothiazoline-6-sulphonate)
DPI	diphenyleneiodonium
DTPA	diethylenetriaminepentaacetic acid
ICP-OES	inductively coupled plasma optical emission spectrometry
LBB	leucoberbelin blue
MCLA	2-methyl-6-(4-methoxyphenyl)-3,7-dihydroimidazo[1,2-a]pyrazin-3-one
MIC	minimum inhibitory concentration
MS/MS	tandem Mass Spectrometry
SAED	selected area electron diffraction
SEM-EDX	scanning electron microscope equipped with an energy dispersive X-ray spectroscopy
SOD	superoxide dismutase
TEM	transmission electron microscopy
XRD	X-ray diffraction
XRF	X-ray fluorescence

Introduction

Wetlands are often considered as sinks for metal contaminants. For example, the Mn content of coastal marshes in the Yellow River of China ranges from 305.87 to 711.39 mg/kg (Sun et al. 2013), while the critical toxicity level of Mn in plants ranges from 200 to 3500 mg/kg (Krämer 2010). Excessive Mn might compete with other cationic metals in terms of metabolism and transport, resulting in nutrient deficiencies of plants (Fernando and Lynch 2015). Based on numerous previous studies, *Suaeda salsa* Pall. is a cash crop halophyte and a promising model organism; it grows in the littoral zone of the Yellow River Delta (Song and Wang 2015; Liu et al. 2018; Guo et al. 2015; Guo et al. 2018; Sui et al. 2017; Wang et al. 2015; Zhou et al. 2016). The species accumulates manganese (Mn), copper (Cu), chromium (Cr), lead (Pb), and arsenic (As) and can therefore be used to remove heavy metals from contaminated wetland sediments (Wu et al. 2012; Li et al. 2012). However, the underlying mechanisms of such pollution removal are still unclear. A striking feature of wetland plants is the presence of plaque on their surface, which is composed of iron and Mn oxides and acts as a source and sink of nutrients and pollutions (Sundby et al. 1998; Khan et al. 2016).

One factor that can affect the metal uptake of wetland plants is the presence of microbial symbionts (Weis and Weis 2004). A study on the submerged plant species *Egeria densa* has revealed that epiphytic bacteria, i.e., *Acidovorax*, *Comamonas*, *Pseudomonas*, and *Rhizobium*, have Mn-oxidizing activities, enabling them to form Mn biofilms on their surfaces (Tsuji et al. 2017). This finding provides new insights into the role of bacteria in the mobilization of Mn (II) in plants. Compared to epiphytic organisms, endophytic organisms form more specific associations with plant tissues (Wani et al. 2015). Recently, several endophytic bacteria with a high Mn tolerance have been discovered, with potential applications in the phytoremediation of Mn-polluted soils (Zhang et al. 2015a, 2015b; Yamaji et al. 2016). However, studies on the underlying mechanisms are scarce.

The oxidation of Mn via non-endophytic bacteria has been studies in the last decade (e.g., Tebo et al. 2005), and different pathways have been proposed. Direct Mn(II) oxidation is catalyzed by multi-copper oxidases (MCOs) (Su et al. 2013; Butterfield et al. 2013; Geszvain et al. 2013), whereas indirect oxidation occurs via the formation of reactive oxygen species (ROS) (Learman et al. 2011; Hansel et al. 2012). The biogenic Mn oxides formed by the different aquatic strains are also diverse. The largest part of the biogenic Mn oxides is represented by hexagonal birnessite [Mn(IV)] (Webb et al. 2005; Miyata et al. 2006), while Mn(III) minerals, also known as bixbyite-like Mn_2O_3, are less common (Zhang et al. 2015c; Hosseinkhani and Emtiazi 2011). In general, biogenic Mn processes require O_2 and therefore occur in the surficial environment (Zhang et al. 2015d; Soldatova et al. 2012; Clement et al. 2009). Under reducing conditions, Mn(II) is mainly converted to rhodochrosite ($MnCO_3$) (Benner et al. 1999).

In this study, we isolated two Mn-oxidizing endophytic bacterial strains from the wetland plant *S. salsa* Pall., with the aim to answer the following questions: 1) can these endophytes affect the Mn accumulation of the host plant? 2) Are the mechanisms of Mn oxidation similar for endophytic and non-endophytic bacteria? To study the Mn accumulation in *S. salsa*, the plant was co-cultivated with the two isolates; Mn content was determined via inductively-coupled plasma optical emission spectrometry (ICP-OES), a scanning electron microscope equipped with an energy-dispersive X-ray

spectroscope (SEM-EDX) and X-ray fluorescence (XRF). The leucoberbelin blue (LBB) test was performed to detect the formation of Mn oxides. To clearify the chemical and molecular mechanisms of Mn oxidation by the two strains, spectra of X-ray diffraction (XRD), energy-dispersive X-ray spectroscopy (EDX), and selected area electron diffraction (SAED) were employed. Subcellular localization of Mn oxides was observed via transmission electron microscopy (TEM). Proteomic analyses, combined with enzymic assays, were also performed to identify the enzymes involved in Mn oxidation. The overall aim of this study was to provide insights into the co-function of endophytic bacteria and plants in biogeochemical Mn cycling in wetland soils.

Materials and methods

Measurement of *S. salsa* pall. Mn concentration

Samples of *S. salsa* Pall. were collected in June 2016 from saline sediment of the Yellow River delta, China (GPS coordinates: N 37° 51′, E 118° 46′). The plants was divided into two groups depending on the prescence or absence of black plaques. Leaves from five plants in each group were mixed and dried at 80 °C for 72 h. Subsequently, the samples were ground into a fine powder, and filtered through a 0.5-mm filter. About 2.0 g of sample was acid-digested with a mixture containing 60% HNO_3 and 60% $HClO_4$ (1:5 *v*/v) and digestion was continued for 2 h. Similarly, the samples of roots and shoots were obtained. The Mn concentrations were analyzed via ICP-OES (IRIS Intrepid II XSP, Thermo Fisher Scientific, MA, USA).

Isolation of endophytic bacteria from *S. salsa* pall

Approximately 5 g of *S. salsa* Pall. leaves were thoroughly rinsed with water to remove sediment and subsequently washed with 100 ml sterile water. The leaves were surface-sterilized by immersion in 0.1% Tween 80 for 3 min, followed by 0.1% $HgCl_2$ for 1 min and 75% (v/v) ethanol for 3 min, before being washed with sterilized H_2O for at least five times. The washed leaves were grounded in a sterilized mortar and 5 ml sterile water were added, followed by incubation at 30 °C for 48 h in Mn-supplemented LB medium containing 10 g l^{-1} peptone, 5 g l^{-1} yeast extract, 10 g l^{-1} NaCl, and 2 mM $MnCl_2$. By using the standard dilution plating technique, the enriched culture was subsequently incubated for 7 d on LB agar supplemented with 5 mM $MnCl_2$. The LB agar contains 10 g l^{-1} peptone, 5 g l^{-1} yeast extract, 10 g l^{-1} NaCl, and 15 g l^{-1} agar. To ensure complete sterilization, 100 μl of the final wash water were spread on LB agar, and no colonies appeared after incubation at 30 °C for 1 week.

Determination of the minimum inhibitory concentration (MIC) of Mn

The cultures of each isolate were incubated in LB broth supplemented with different concentrations of $MnCl_2$ (0, 10, 20, 30, 35, 40, 45, 50, and 60 mM) at 30 °C and shaken at 150 rpm for 72 h. Growth was monitored by optical density at 600 nm using a spectrophotometer. The lowest Mn concentration that inhibited growth was considered as the MIC.

Mn-oxidizing assay

Leucoberbeline blue (LBB) staining (Krumbein and Altmann 1973; El Gheriany et al. 2009) was carried out as described by Krumbein and Altmann (1973). Briefly, 300 μl of each sample were incubated with 60 μl of Leucoberbelin Blue 1 (Sigma, 0.04%, *w*/*v*) and 900 μl of acetic acid (45 mM) for 2 h at 30 °C. The reaction was monitored based on the optical density at 620 nm using a spectrophotometer. Standard curves were prepared with $KMnO_4$ and LBB, and the results are expressed as Mn(IV) oxide equivalents.

To determine the intercellular Mn-oxidizing activity of the strains, cell-free extracts were prepared. The strains were grown to the stationary phase in K media supplemented with 2 mM $MnCl_2$ at 30 °C and 150 rpm. The K medium (1 L) was composed of 2 g peptone, 0.5 g yeast extract, 0.56 g KCl, 7.24 g $MgSO_4 \cdot 7H_2O$, 0.83 g $CaCl_2$, and 10 g NaCl. Cells were harvested by centrifugation for 15 min at 6000 rpm and 4 °C, washed in 100 ml HEPES buffer (20 mM, pH 7.0), recentrifuged, and resuspended in 15 ml HEPES buffer (20 mM, pH 7.0). The mixture was sonicated for 30 min at 20 kHz. The cell-free extract was obtained via collection of the supernatant after centrifugation (8000 rpm for 30 min at 4 °C). To determine extracellular activity, the strain was grown in K media at 30 °C for 10 d, and the supernatant was collected and precipitated by 70% saturation of ammonium sulfate. The protein precipitates

were dissolved in HEPES buffer (pH 7.0) and dialyzed against the same buffer. The LBB assays were carried out as described above. To test the effects of the components on Mn-oxidizing activity, fresh stocks of various coenzymes, metal ions, and inhibitors were added to the assay mixture.

Identification of Mn-oxidizing bacteria by 16S rRNA sequencing

The Mn-oxidizing isolates were grown in LB medium supplemented with 2 mM $MnCl_2$ for 24–72 h at 30 °C while shaking at 160 rpm. Genomic DNA from each isolate was extracted using a DNA isolation kit (BioTeke, Beijing, China) according to the manufacturer's protocol. The 16S rRNA gene sequence of the strains was amplified using Taq DNA polymerase and the primer pair 27F (5'-AGAGTTTGATCCTG GCTCAG-3′) and 1492R (5'-TACGGCTACCTTGT TACGACTT-3′). The reaction products were purified with a kit (BioTeke, Beijing, China) and sequenced by BioSune (Shanghai, China). The 16S rRNA sequences were aligned with the BLAST algorithm (Altschul et al. 1990) and the EzTaxon-e service (Kim et al. 2012) and submitted to GenBank. Multiple sequence alignments were analyzed using CLUSTAL_X 2.0 (Larkin et al. 2007). The phylogenetic trees were constructed by the neighbour-joining method (NJ, Saitou and Nei 1987) using the MEGA 6 software (Tamura et al. 2013). Evolutionary distances were calculated according to the Kimura two-parameter model (Kimura 1980). Branch support was calculated by bootstrap analysis.

Cultivation of *S. salsa* pall. In the laboratory

Individuals of *S. salsa* Pall. were precultured in Hoagland solution at pH 6.0 at a temperature range of 25–28 °C for 10 d.The nutrient solution was replaced every 3 d, and the endophytic bacteria were cultured in 100 ml LB liquid medium for 48 h at 30 °C and 150 rpm. Cells were collected via centrifugation, and the precipitates were washed three times with distilled water. Subsequently, *S. salsa* Pall. plants were exposed to 200 μM $MnCl_2$ in Hoagland solution. Each endophytic bacterial strain was inoculated with the plants at a final density of 10^6 CFU ml^{-1}, and the non-inoculated pot was considered as a control.

Analysis of elements on the surface of *S. salsa* pall. Plants

Surface elements of the collected plants were analyzed with a scanning electron microscope equipped with SEM-EDX, according to a previously described method (Michalak et al. 2011). For this, the root or leaf segments were mounted on an aluminum stub with glue and subsequently gold-sputtered at 15 mA for 60 s. Afterwards, they were monitored via an SU8010 (Hitachi, Japan) equipped with an EDX spectral detector (Model 550i). The accelerating voltage during monitoring was 20 keV. In addition, XRF was applied to detect Mn. The black plaques were cut down from the roots with a sterilized knife and ground in a mortar, followed by oven-drying at 60 °C for 2 d. Elemental intensities were determined in the Shandong Analysis and Test Center (Jinan, China) via XRF spectrometry (ZSX Primus II, Japan).

XRD analysis of biogenic Mn formed by endophytic bacteria

Strains were grown at 30 °C for 10–12 d in K medium supplemented with 2 mM $MnCl_2$. Cell-free or extracellular extracts were collected and incubated with 0.1 M $MnCl_2$ at 37 °C for 24 d. For XRD, the precipitates of the incubation were centrifuged at 3000×g for 10 min and subsequently air-dried to obtain 100 mg of powder. The samples were analyzed a Bruker D8-Advance X-ray diffractometer (Bruker AXS, Germany) and scanned across the range of 2θ from 10° to 85°. The analysis was conducted with Cu Kα (λ = 0.15418 nm) at 40 mA and 40 kV, with a step size of 0.02° and a scan speed of 10°/min. Patterns were analyzed using the JADE 6 (Materials Data, Inc., USA) software and identified according to the International Center for Diffraction Data (ICDD) PDF-2 database (http://www.icdd.com/).

TEM analysis of Mn oxides formed by endophytic bacteria

The bacterial strains were incubated at 30 °C for 7 d in liquid K medium supplemented with $MnCl_2$ (2 mM). For electron microscopy studies of the microspherical traits of the biogenic deposits formed by the strains, cell-mineral pellets were collected by centrifugation at 4000×g for 15 min and fixed with 3.0% glutaraldehyde, followed by washing with 0.1 M phosphate-buffered

saline (PBS) buffer for three times, staining with 1.0% OsO_4 for 1 h, and washing with PBS buffer for another three times. Four dehydration steps with 30, 50, 70, and 90% ethanol and absolute dehydration with propylene oxide were carried out prior to embedding with araldite resin (2:1, 1:2, and 100% propylene oxide: araldite). The samples were cured at 60 °C before slicing to a 70-nm thickness and staining with 3.0% uranyl acetate and lead citrate. The ultra-microtome sample was then investigated via a JEM-1200EX microscope. The EDX and SAED were carried out to obtain the elemental and structural information. Samples were coated with amorphous carbon and analyzed using a JEOL 2100F microscope (JEOL, Tokyo, Japan) at 200 kV, equipped with an Oxford X-Max 80 T EDX system (Oxford Instruments, Oxford, UK).

Antioxidant activity assay towards ABTS

The antioxidant activity assays were determined at 30 °C using ABTS, [2,2-azinobis-(3-ethylbenzothiazoline-6-sulphonate), Sigma, USA] as substrate according to the previously described method (Bohu et al. 2015). The oxidation rate of the substrate was detected by determining absorbance at 420 nm using a Purkinje TU-1810 UV-VIS spectrophotometer (Beijing Purkinje General Instrument, Beijing, China).

Protein purification and proteomic MS/MS analysis

Strains were grown in K medium at 30 °C and 150 rpm for 7 d. The crude proteins of *P. composti* SS02 were prepared via collecting the supernatant of the culture, while the crude protein of *P. eucrina* SS01 was obtained by collection of the supernatant from centrifugation (8000 rpm for 30 min at 4 °C) after the cells were sonicated. The proteins in the supernatant were precipitated by adding ammonium sulfate powder at a final concentration of 70%. The precipitates were collected by centrifugation (8000 rpm, 15 min) and dissolved in 50 mM Tris-HCl buffer (pH 7.0), followed by being placed in a DEAE-Sepharose Fast Flow chromatography column pre-equilibrated with the same buffer. The column was then eluted with a linear gradient of 0 to 1.0 M NaCl, and the Mn(II) oxidation activities of the fractions were determined by using the LBB method as described previously. The active fraction was collected for the analysis of 10% SDS-PAGE. The bands of interest were excised from the gel, digested with trypsin, and sent to Biosune (Shanghai, China) for peptide sequencing, using the UltrafleXtreme MALDI TOF/TOF instrument (Bruker Daltonics, Bremen, Germany).

Detection of uperoxide production

Superoxide was detected with the chemiluminescent probe MCLA (2-methyl-6-(4-methoxyphenyl)-3,7-dihydroimidazo[1,2-a]pyrazin-3-one), following the protocol established by Learman et al. (2011). Briefly, basic luminescence was calculated by preparing a mixture of xanthine (50 μM) and diethylenetriaminepentaacetic acid (DTPA, 100 μM) and 280 μl of the purified active solution parts collected after DEAE-Sepharose chromatography. A blank measurement was performed by adding SOD (50 kU/l) to the above mixture to remove superoxide. The superoxide production of the sample was monitored by adding 12.5 μM of MCLA to the basic mixture and reaching the steady stage after 5 min.

Results

Mn accumulation in *S. salsa* pall

In June, we collected plants of *S. salsa* Pall. from the coastal area of the Yellow River, China. In one group (G1), a layer of black plaques was observed on the surface of roots and stems (Fig. 1a), while the other group (G2) showed no such layer (Fig. 1a). Dissection of plants from G1 revealed that black precipitates also appeared in the inner tissues, known as pith (Fig. S1A). In LBB staining, roots from G1 showed a blue color, while the roots from G2 were colorless (Fig. 1b). This suggests that the black plaques from G1 contained Mn oxides (Krumbein and Altmann 1973; El Gheriany et al. 2009). Based on the results of the SEM-EDX analysis, the plaque contained Mn, C, O, Cl, and K (Fig. 1d, e). Similarly, analysis of the black precipitates in the pith confirmed the presence of Mn, Fe, C, and O (Fig. S1C, D). Although there was no visible black precipitates on the leaves of *S. salsa* Pall., the LBB test was positive for the leaves from individual plaque-covering plants, indicating the accumulation of Mn oxides on the surface of leaves. In contrast, the test was negative for non-covered plants (Fig. 1b). These results suggest that Mn oxides are accumulated as dark precipitates on both belowground and aboveground tissues of *S. salsa* Pall.

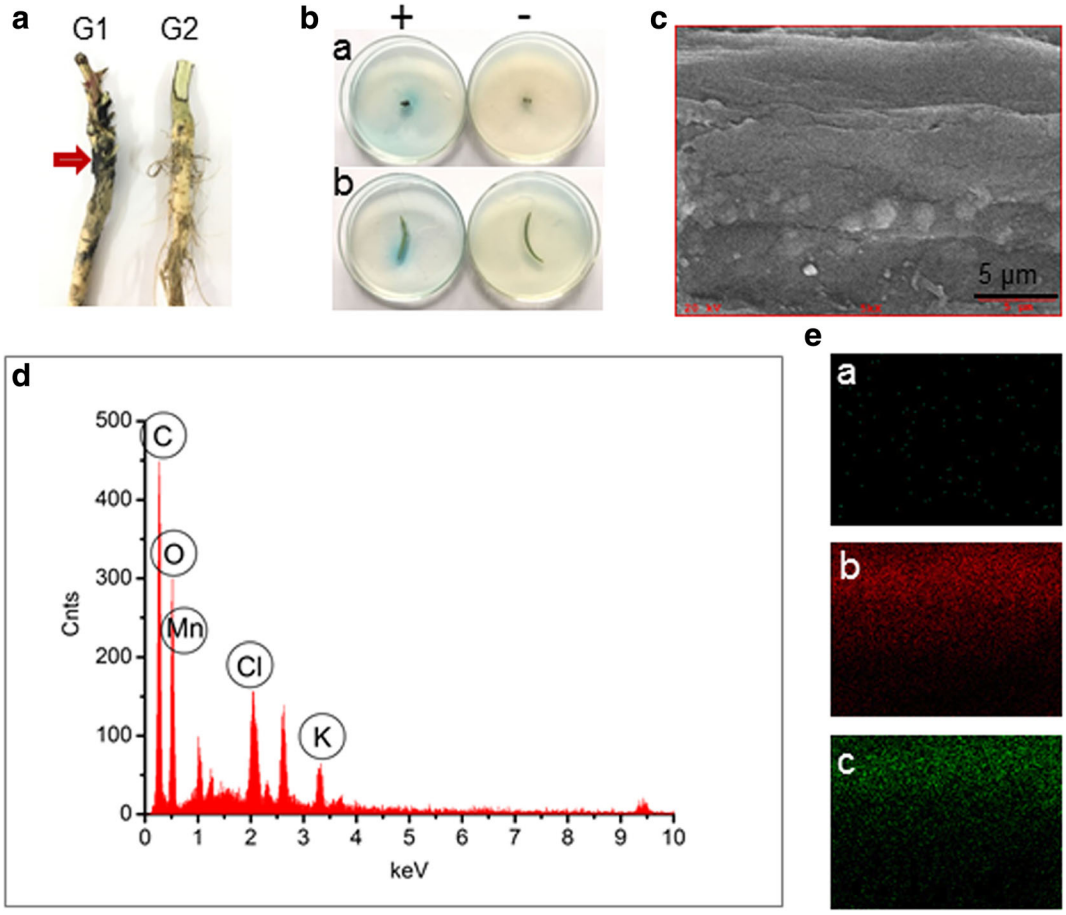

Fig. 1 Precipitation of Mn-containing plaques on the surface of *Suaeda salsa* Pall. A, Field collected *S. salsa* Pall. with (G1) and without (G2) visible black plaques on the surface of the root. A segment of root with black precipitations (indicated by red arrow) was mounted onto an aluminum stub for SEM-EDX analysis. B, LBB staining of the root (**a**) and leaf (**b**) from *S. salsa* Pall. with (+) and without (−) visible black plaques. C, SEM view of the root with a location indicated by the arrow in Fig. A. D, Elemental analysis by EDX of the surface of the analyzed region (as showed in Fig. C) showing the appearance of several metals, including Mn. E. Individual EDX elemental distribution maps for Mn (a), C (b),and O (c)

We also measured the Mn concentrations in different tissues of *S. salsa* Pall. via ICP-OES. For plants from G1, the Mn concentrations of the root, shoot, and leaves were 14, 9 and 10 mg/kg, respectively (Fig. S2). By comparison, plants from G2 contained lower amounts of Mn, namely 9, 4, and 4 mg/kg for root, shoot, and leaves, respectively (Fig. S2). These results indicate that the presence of black precipitates was associated with elevated Mn concentrations in the tissues of *S. salsa* Pall.

Isolation and identification of Mn-oxidizing endophytic bacteria from *S. salsa* pall

By cultivation in LB medium supplemented with 5 mM $MnCl_2$, a total of three isolates were cultured from *S. salsa* Pall. plants coated with black plaques (G1). The three strains were tolerant to $MnCl_2$ at a range from 10 to 45 mM (Table 1). Two of these isolates, strain SS01 and SS02, had Mn(II)-oxidizing activity as indicated by LBB staining. Strain SS01 exhibited an activity of 585 μM of the equivalent MnO_2, whereas strain SS02 had a relatively lower activity at 169 μM (Table 1). Sequences of the amplified 16S rRNA of the two strains showed that they belonged to the genera *Pantoea* and *Pseudomonas*. Strain 1 showed 100% similarity of the 16S rRNA sequence with *Pantoea eucrina* PSNIH1 (GenBank no. CP009880) and thus was identified as *Pantoea eucrina* SS01. Strain 2 was ascribed to *Pseudomonas composti* SS02 as the 16S rRNA sequence showed 99% similarity with *Pseudomonas composti* CCUG 59231 (GenBank no. FOWP01000025). The third endophytic isolate, *Enterobacter* sp. SS03,

Table 1 Identification, description and Mn-oxidizing ability of endophytic bacteria isolated from *Suaeda salsa* Pall

Isolate*	Accession no.	Gene annotation of the top-hit strain (accession no.) #	Identity (%)	MIC (mmol/l)	Mn(II)-oxidizing activity (MOA) of formed MnO_2 (μM) †	Intercellular MOA activity	Extracellular MOA activity
SS01	MF086656	*Pantoea eucrina* PSNIH1 (CP009880)	100	30	586	+	–
SS02	MF086658	*Pseudomonas composti* CCUG 59231 (FOWP01000025)	99	10	169	w	+
SS03	MF086659	*Enterobacter aerogenes* KCTC 2190 (CP002824)	99	45	0	–	–

*Isolates were selected by cultivation with 5 mM Mn(II) supplemented in LB medium

By alignment using the BLAST algorithm (Altschul et al. 1990) and the EzTaxon-e service (Kim et al. 2012). Uncultured bacteria were manually removed

† Strains were grown in K media supplemented with 2 mM $MnCl_2$ at 30 °C for 7 d

+ positive, − negative, w weak

presented a high tolerance to $MnCl_2$ at 45 mM, but its LBB test was negative (Table 1, Fig. S3).

Phylogenetic analysis of the reported Mn-oxidizing strains illustrated that the two isolates were both clustered within the Gammaproteobacteria phylum of the class Proteobacteria (Fig. 2), which includes several model Mn-oxidizing bacteria that have been isolated from aquatic areas, such as *Roseobacter* sp. AzwK-3b (Learman et al. 2011), *Aurantimonas manganoxydans* SI85-9A1 (Anderson et al. 2009) and *Leptothrix discophora* SS-1 (Adams and Ghiorse 1986). Moreover, the two isolates were clustered together with a short phylogenetic distance and were separated from those above-mentioned marine bacteria.

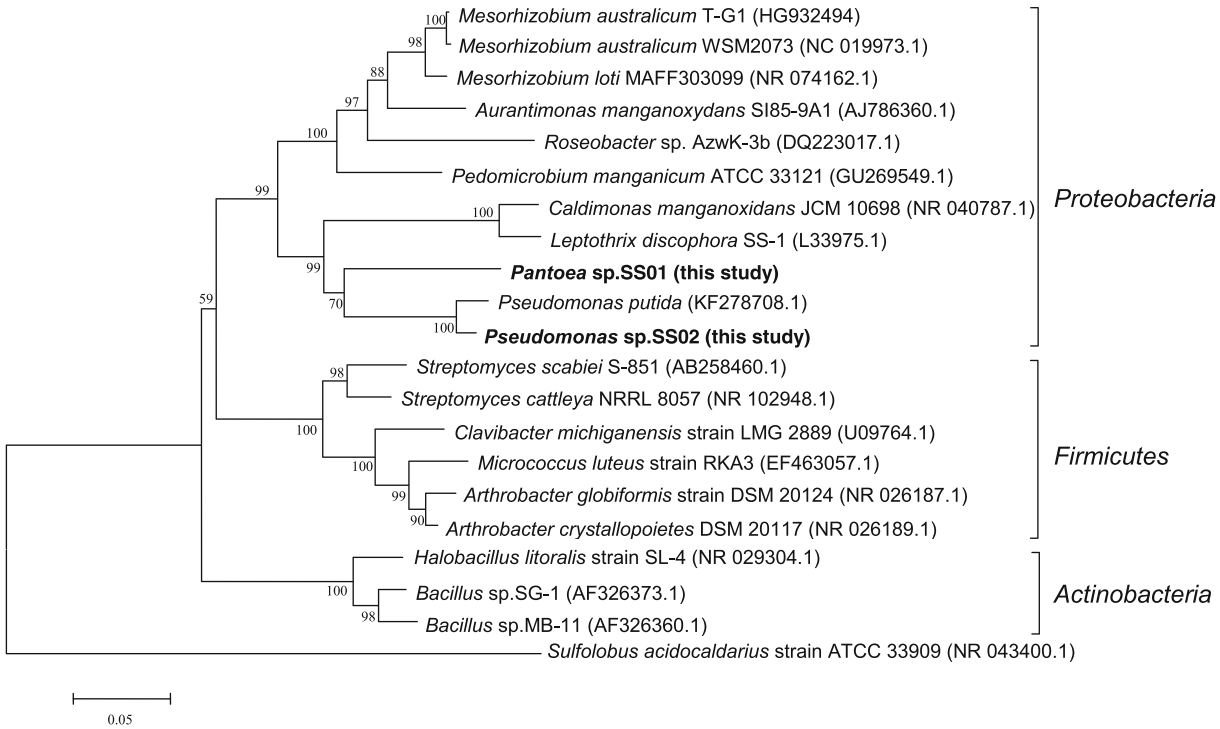

Fig. 2 The neighbour-joining (NJ) tree based on 16S rRNA gene sequences of Mn(II) oxidizing bacteria (MOB) isolated in this work (indicated by boldface type) and previously reported MOB strains. The 16S rRNA sequence of *Sulfolobus acidocaldarius* strain ATCC 33909 was used as an outgroup. Bootstrap values are expressed as percentages of 1000 replications, and only bootstrap values above 50% are shown. GenBank accession numbers are given in parentheses. Bar, 0.05 substitutions per nucleotide

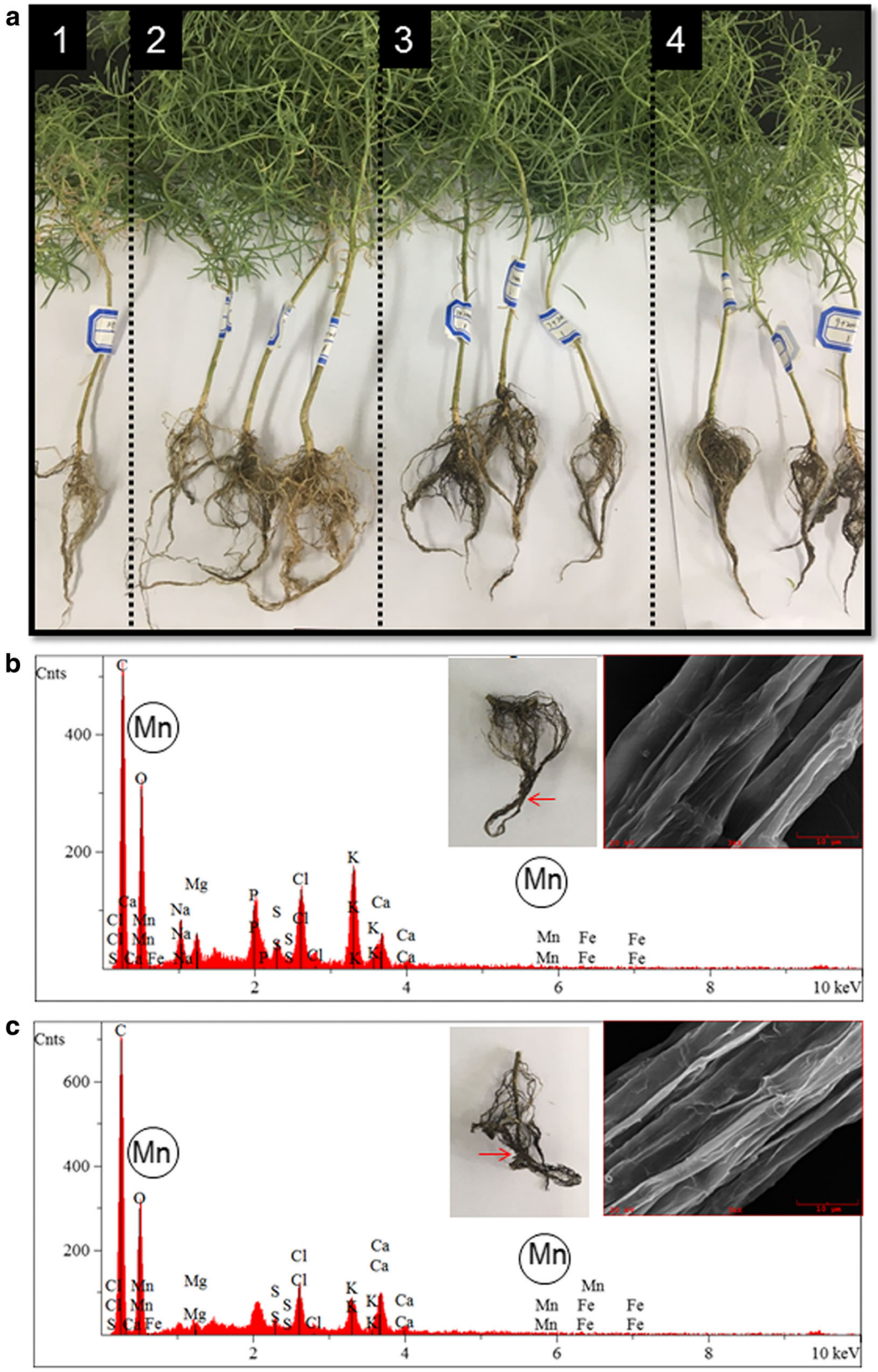
a
1
2
3
4
b
Cnts
400
200
C
Mn
O
Mg
P
S
Cl
K
Ca
Na
Fe
2
4
6
8
10 keV
c
Cnts
600
400
200
C
Mn
O
Mg
S
Cl
K
Ca
Fe
2
4
6
8
10 keV

◀ **Fig. 3** Mn precipitation on the root of laboratory-cultivated *S. salsa* Pall. A, Photographs of laboratory-cultivated *S. salsa* Pall. plants. 1, plant cultured by Hoagland solution for 30 d; 2, plants exposed to 200 μM $MnCl_2$ in Hoagland solution for 30 d; 3, plants co-cultured with *P. eucrina* SS01 and Hoagland solution with 200 μM $MnCl_2$ for 30 d; 4, plants co-cultured with *P. composti* SS02 and Hoagland solution with 200 mM $MnCl_2$ for 30 d. B, Elemental analysis by EDX of the surface of root from plant co-cultured with *P. eucrina* SS01 (as indicated by the arrow in inset). C. Elemental analysis by EDX of the surface of root from plant co-cultured with *P. composti* SS02 (as indicated by the arrow in inset)

Mn precipitation on laboratory-cultivated plants mediated by the bacteria

Black precipitates are rarely reported in plants cultivated under laboratory conditions (Tsuji et al. 2017). In this work, we observed that when *S. salsa* Pall. plants were cultured with 200 μM $MnCl_2$ for 30 d, a few roots turned black, whereas most of the plants showed no apparent symptoms (Fig. 3). However, when plants were co-cultured with Mn-oxidizing endophytic bacteria and 200 μM $MnCl_2$ for 30 d, black precipitates were clearly observed on the surface of all roots (Fig. 3). The LBB staining of black precipitates was positive, suggesting the accumulation of Mn oxides. Further, SEM-EDX analysis showed that the precipitates were composed of Mn, in addition to C, O, K, Cl, P and other elements (Fig. 3). The XRF also showed the presence of Mn in the black precipitates of the plants cultivited with strains SS01 and SS02, whereas no Mn signal could be detected for untreated plant roots (Fig. S4). These results indicate the involvement of endophytic Mn-oxidizing bacteria in the accumulation of Mn oxides in *S. salsa* Pall.plants.

Characterization of the chemical composition of biogenic Mn oxides

For *P. eucrina* SS01, TEM revealed the presence of 50-nm-thick and rounded deposits of electron-dense material in the membranes of the cells (Figs. 4a, S5A). According to the results of the EDX analysis, the deposits were mainly composed of Mn, C, and O (Fig. 4Ca). However, electron diffraction of deposits formed by *P. eucrina* SS01 showed no visible diffraction spots (Fig. 4Cb, inset), probably because of the effects of cells or cell membranes mixed with the Mn minerals. As depicted in Fig. 4e, the XRD patterns of the Mn aggregates from *P. eucrina* SS01 exhibited five distinct peaks at angles of 23.8°, 30.7°, 40.7°, 44.5°, and 50.5° corresponding to $MnCO_3$ (JCPDS 44–1472) (Fig. 4Ea), as well as two peaks at 27.7°, and 37.1° (Fig. 4Eb), typical for MnO_2 (JCPDS 44–0142).

For *P. composti* SS02, the precipitation of non-transparent and irregular deposits was only observed away from the cells (Figs. 4b, S5B), indicating an extracellular reaction. The EDX showed that deposits were also composed of Mn and O along with other elements (Fig. 4 Da). The SAED pattern analysis showed that diffraction spots were arranged as continuous rings (Fig. 4Db, inset), suggesting that the deposits were heteromorphic and crystallographic. The XRD pattern of Mn deposits of *P. composti* SS02 showed two main peaks at 33.5° and 55.4° (Fig. 4Fb), representing Mn_2O_3 (JCPDS 41–1442). The presence of $MnCO_3$ was also confirmed by five typical peaks at 24.3°, 31.2°, 37.3°, 41.3°, and 51.5° (Fig. 4Fa,Ga, JCPDS 44–1472). Additionally, the intense peaks at 31.8° and 45.5° indicated the presence of NaCl (Fig. 4Fc,Gc, JCPDS 05–0628).

Molecular mechanisms involved in the Mn(II) oxidation

The different locations and compositions of the minerals from the two strains indicate distinct mechanisms of bacterial Mn(II) oxidation. To confirm this, we performed LBB analysis to examine the intercellular and extracellular Mn-oxidizing activities in *P. eucrina* SS01 and *P. composti* SS02. In *P. eucrina* SS01, Mn-oxidizing activity was detected only in the cell lysate, whereas the activity of *P. composti* SS02 occurred extracellularly (Table 1). These results were in line with the TEM observations (Fig. 4a, b), suggesting that Mn(II) oxidation occurred in the different locations of cells of the two strains.

Furthermore, the molecular mechanism of Mn oxidazation was studied. The effect of chemicals on the Mn(II) oxidation was investigated. For *P. eucrina* SS01, addition of NADH (400 μM) stimulated activity (1.4-fold), while SOD (15 kU) decreased the activity (Table S1). It should be noted that NADH is a substrate of NADH-oxidase and incrases superoxide (O_2^-) production (Vinogradov and Grivennikova 2005), whereas SOD serves as a scavenger of reactive oxygen species (ROS) (Learman et al. 2011). These results suggest that the formation of Mn oxides of *P. eucrina* SS01 might be associated with ROS generation (Learman et al. 2011). Moreover, the addition of the oxidoreductase inhibitor diphenyleneiodonium (DPI) quenched 50% of the Mn(II)-oxidizing activity (Fig. 5a). In a previous study,

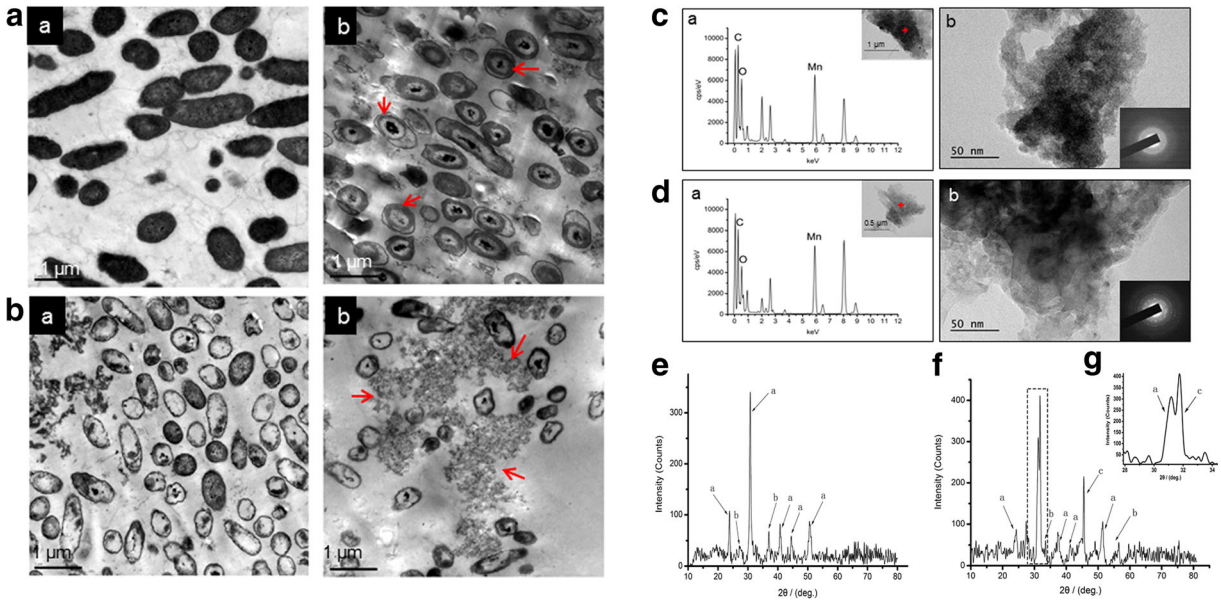

Fig. 4 The subcellular localization and chemical composition of biogenic Mn oxides obtained by the endophytic bacterial strains. A,B, TEM views of the ultrastructures of *P. eucrina* SS01 (A) and *P. composti* SS02 (B) cells with (a) or without (b) incubation of $MnCl_2$. Strains were incubated in K media supplemented with 2 mM $MnCl_2$ at 30 °C for 7 d. Arrows indicate the electron-dense of Mn deposits. C,D, TEM analysis of the Mn deposits produced by *P. eucrina* SS01 (C) and *P. composti* SS02 (D) cells. a. Elemental analysis by EDX of the minerals formed by the strains. +, Corresponding selected area for EDX analysis. b. TEM micrograph of a cluster of Mn minerals and corresponding selected area diffraction patterns. E, XRD pattern of $MnCO_3$ (a) and MnO_2 (b) produced by *P. eucrina* SS01. F, XRD pattern of Mn_2O_3 (a), $MnCO_3$ (b), and NaCl (c) produced by *P. composti* SS02. G, an amplification of peaks indicated in the dashed quadrilateral area in Fig. F

DPI inhibited peroxidase-mediated superoxide (O_2^-) production (Minibayeva et al. 2001). In our study, we observed the production of NADH-stimulated superoxide in strain SS01. We tried to isolate and purify the proteins responsible for Mn oxidization in strain SS01, and the active components were tested by LBB staining and collected after DEAE-Sepharose chromatography; however, SDS-PAGE showed that the band of the active parts was weak (Fig. 5d), and was identified as catalase by mass spectrometry (Table 2). Since previous studies showed that the ROS mediates Mn(II) oxidation via a variety of ROS scavengers (Learman et al. 2011), we assumed that the purified catalase might function as a chemical scavenger in detoxification of the intracellular ROS, and participated in the Mn oxidation indirectly. Previous works have identified the ROS-mediating Mn(II) oxidation compound as superoxide (Learman et al. 2011, 2013). Thus, we detected superoxide in the collected active component by adding MCLA, a superoxide-specific chemiluminescent probe (Godrant et al. 2009; Learman et al. 2011). The significantly increased chemiluminescence intensity indicated the reaction of MCLA with superoxide (O_2^-) (Fig. 5b). These results strongly suggest that superoxide (O_2^-) plays an important role in Mn oxidization of strain SS01.

For *P. composti* SS02, the addition of NADH had no significant effect on the Mn-oxidizing rate (Table S1). However, the addition of 10 μM coenzyme Q, a chemical that decreases the oxidative stress of cells and increases the expression of antioxidant parameters such as superoxide dismutase and catalase, significantly increased the oxidation rate by 1.3 times (Table S1). In addition, DPI (100 μM) reduced 53% of the Mn(II)-oxidizing activity (Fig. 5a). Thus, the results suggest a correlation between Mn oxidization and ROS in strain SS02, but the mechanism was probably different that for strain SS01. Moreover, Cu^{2+} (100 μM) increased the oxidation rate of the cells by 1.4 times (Fig. 5a; Table S1), and the antioxidant activity of strain SS02 against ABTS was 0.296 OD^{-1} ml^{-1}, whereas the ABTS activity (0.030 OD^{-1} ml^{-1}) of strain SS01 was neglectable (Fig. 5c). Furthermore, the proteins of strain SS02 were separated by DEAE-Sepharose chromatography, and the active band was identified as catalase-peroxidase by mass

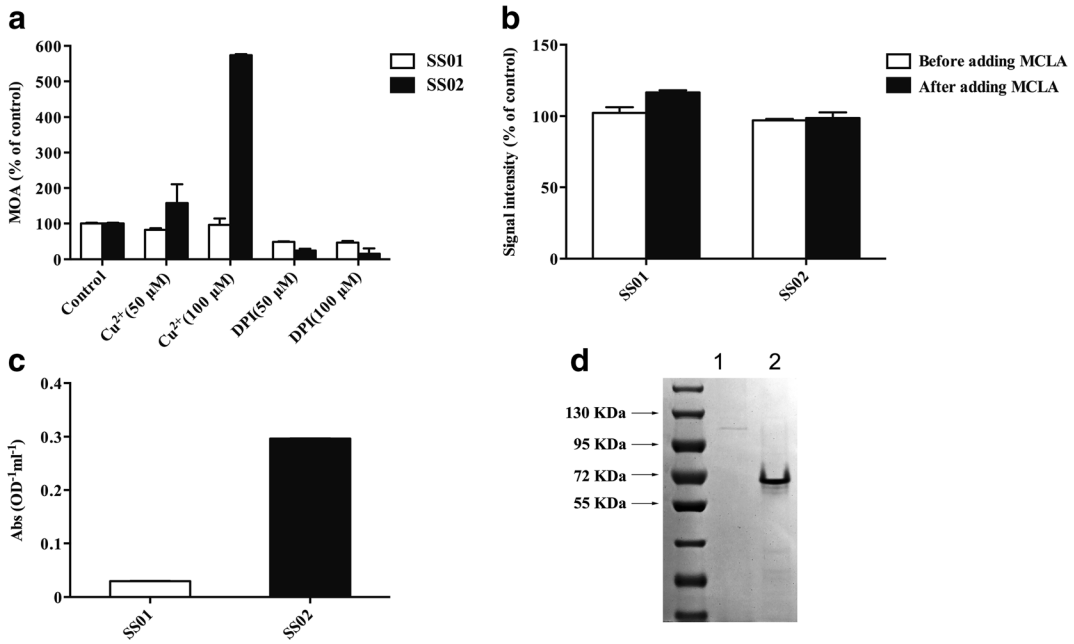

Fig. 5 The enzyme assays and purified proteins. A, The Mn(II)-oxidizing activities of *P. eucrina* SS01 (white bars) and *P. composti* SS02 (black bars) under different chemicals. Experimental data normalized to control, the standard condition with no added chemicals. Concentrations of Mn oxides were determined using LBB (Krumbein and Altmann 1973). B, The superoxide production by *P. eucrina* SS01and *P. composti* SS02. Luminescences was calculated by adding 12.5 μM of MCLA to basic mixtures containing 50 μM xanthine, 100 μM DTPA, and 280 μl of the active solutions collected after DEAE-Sepharose. Experimental data normalized to the blank measurement by adding SOD (50 kU/l) to the basic mixtures to remove superoxide. C, The ABTS activities of *P. eucrina* SS01 and *P. composti* SS02. Activities were determined at 30 °C using 0.5 mM ABTS as substrate. D, The active protein parts from *P. eucrina* SS01 (1) and *P. composti* SS02 (2) that were collected after DEAE-Sepharose, and were analyzed by 10% SDS-PAGE. The activities of the protein solutions were determined by LBB methods

spectrometry (Table 2), which is consistent with the ABTS and DPI tests. The active protein solutions also showed a 3-fold increase in the Mn(II)-oxidizing activity when Cu^{2+} (100 μM) was added (Fig. 5a), further indicating the differential Mn oxidizing mechanisms between strain SS01 and strain SS02.

Discussion

Wetlands can represent sinks for heavy metals and other pollutants, thereby providing important phytoremediation services. The fate of heavy metals within plant tissues is critical in the circulation of

Table 2 MS/MS peptide identification of the protein bands in filtrate active for Mn(II) oxidation

Isolates	Protein locus[a]	Protein description	Estimated MW (kDa)[b]	Total spectral counts[c]
SS01	A0A1X1DHL6	Catalase	55	150
SS01	A0A1X1DJZ7	ATP-binding protein	56	48
SS01	A0A1X1DT32	Two-component system response regulator	27	43
SS02	A0A1I5S769	Catalase-peroxidase	78	43
SS02	A0A1I5PWF7	Pyridoxine/pyridoxamine 5′-phosphate oxidase	24	42
SS02	A0A1I5QW64	Putative protein	7	39

[a] GenBank designation

[b] Molecular weights were estimated based on amino acid sequences

[c] For counts, peptide probability was set at >95%, and protein probability was set at >99.9% using Scaffold, minimum of 2 peptides

elements within wetlands (Weis and Weis 2004). Manganese is an essential constituent of PSII during oxygenic photosynthesis, but at high concentrations, it restricts plant growth (Fernando and Lynch 2015). The oxidation of Mn is a profound way to reduce the Mn toxicity of this heavy metal, and the oxidizing process in situ is considered to involve fungi and bacteria (Spiro et al. 2009). However, the interactions between plants and Mn-oxidizing bacteria are still unclear. Recent studies have focused on the physiological factors of plants in Mn uptake, transport, and release (Fernando and Lynch 2015), whereas the effectiveness of microbial symbionts in this process has not been clarified so far. In this study, we isolated three Mn-tolerant endophytic strains from the leaves of *S. salsa* Pall. by a culture-based approach. Among these isolates, two Proteobacteria strains, *Pantoea eucrina* SS01 and *Pseudomonas composti* SS02, were found to have Mn-oxidizing abilities. Previous studies have shown that *Pseudomonas* strains could be divided into non-Mn-oxidizing and Mn-oxidizing families (Jung and Schweisfurth 1979; Geszvain et al. 2013). The strain *P. composti* SS02, which has also been isolated from salt marshes in heavy metal-contaminated areas (Andrades-Moreno et al. 2014), is a new member of Mn-oxidizing *Pseudomonas*. In comparison, *P. eucrina* SS01, isolated in this work is a novel Mn-oxidizing bacterial strain, and the role of the genus *Pantoea* in Mn oxidation has not been studied.

So far, most Mn(II)-oxidizing bacteria have been isolated from aquatic environments; only a few works were conducted in terrestrial environments (Zhang et al. 2015c). Several Mn-oxidizing strains of epiphytic bacteria have been found on the surface of field-collected *E. densa* plants, affecting Mn accumulation (Tsuji et al. 2017). However, for none of the endophytic bacterial species, Mn oxidization has been observed. The discovery of two Mn-oxidizing endophytic bacterial strains from *S. salsa* Pall. significantly contributes to our knowledge of the habitat and diversity of Mn-oxidizing bacterial species.

Although the presence of plaques composed of iron and Mn oxides have been enigmatically reported on the surface of wetland plants (Mendelssohn and Postek 1982; Vale et al. 1990), yet few studies have clarified the morphology and composition of these metal-rich rhizoconcretions (Sundby et al. 1998; Weis and Weis 2004) and the mechanism underlying their formation is unclear. In this study, we observed black precipitations from the wetland plant *S. salsa* Pall. collected from wild habitat, as well as from the laboratory-cultivated plants. We also showed that the black precipitations appeared not only on the surface of the root but also in the pith of the plants. LBB staining and SEM-EDX analysis further indicated that Mn oxides present in the precipitations. A previous study has suggested that the production of biogenic Mn oxides in biofilms on the epidermis of an Mn hyperaccumulator plant, *Egeria densa*, can elevate Mn levels inside the plants (Tsuji et al. 2017). In this study, however, the concentrations of Mn in the leaves, stems, and roots of *S. salsa* Pall. with deposition of biogenic Mn on the surface were all below 20 mg/kg, higher compared with the Mn concentrations of tissues from *S. salsa* plants without Mn deposits, but far below the level of 10,000 mg/kg found in Mn-hyperaccumulating plants (Fernando et al. 2010). Although the production of Mn might be influenced by the growth state, the season, and other environmental parameters, we can argue here that *S. salsa* Pall. is not an Mn hyperaccumulator. In Mn hyperaccumulators, Mn predominates in its lowest (+2) oxidation state (Fernando et al. 2010). Excess Mn(II) is sequestered and detoxified in dermal tissues of these plants (Fernando et al. 2013), although there is no clear explanation for detoxification in these tissues. We assume that, in contrast to the strong absorption of Mn by Mn hyperaccumulating plants, *S. salsa* Pall. might survive by the formation of iron and manganese oxides on its surface to reduce the harshness of excess Mn and to prevent the uptake of other heavy metals from saline and contaminated soils. Numerous studies have shown that *S. salsa* is an effective phytoremediation of salt marshes by reducing toxic metal levels from saline soils (Brown et al. 1999; Li et al. 2011). This process might be facilitated by the formation of Mn plaques on the surface of the plants, probably in combination with the activity of endophytic bacteria. These findings improve our understanding of the organic geochemistry in salt marshes and provided new insights into the co-functions of microbes and plants in this process.

As indicated in the XRD and SAED patterns, the biogenic Mn oxides produced by the two endophytic strains differ significantly: birnessite (MnO_2) and rhodochrosite ($MnCO_3$) are produced by the endophytic *P. eucrina* SS01, while the bixbyite-like mineral (Mn_2O_3) and $MnCO_3$ are formed by *P. composti* SS02. These results imply that diverse mechanisms of Mn-oxidation are involved in endophytic bacteria. So far, microbially mediated Mn(II) oxidation processes have

mainly been studied in four typical marine strains, *Roseobacter* sp. AzwK-3b, *Leptothrix discophora* strain SS-1, *Bacillus* sp. strain G-1, and *Pseudomonas putida* strains MnB1 and GB-1 (Andeer et al. 2015; Corstjens et al. 1997; Dick et al. 2008; Geszvain et al. 2013). The primary Mn oxides produced by these bacteria were exclusively hexagonal birnessite with the presence of MnO_2. Other forms of Mn oxides have rarely been studied, whereas a low-valence biogenic Mn oxide, Mn_2O_3, has been reported in two strains, *Acinetobacter* sp. and *Bacillus* CUA (Hosseinkhani and Emtiazi 2011; Zhang et al. 2015c).

We suggest the existence of various underlying Mn oxidation mechanisms for the two endophytic bacteria. The effects of the chemicals described in this work revealed that Mn-oxidizing activities are a correlated with ROS in both strains. However, superoxide appears to be associated with the formation of MnO_2 by *P. eucrina* SS01, whereas superoxide was not detected in *P. composti* SS02. Catalase was identified in the Mn-oxidation active part in strain SS01, while catalase-peroxidase was found in strain SS02, which is consistent with the positive ABTS results for strain SS02 and the negative results for strain SS01. Since heavy metals generate ROS, leading to oxidative stress (Pinto et al. 2003), the induction of these hydrogen peroxide-detoxifying enzymes might be a physiological response to oxidative stress in the cells of these endophytic bacteria.

In this paper, we show the appearance of Mn oxides as plaques on the surface and in the pith of a wetland plant, *S. salsa* Pall. Two endophytic bacterial strains capable of oxidizing Mn(II) were isolated from these plants. Laboratory cultivation of *S. salsa* Pall. and the two isolates showed enhanced precipitation of Mn oxides on the plant roots, possibly serving as an oxidant of heavy metals and pollutants and as a scavenger of trace nutrients to sustain the growth of *S. salsa* plants in saline and heavy metal-contaminated wetlands. The chemical compositions of Mn were different for the two strains, and we suggest the presence of ROS-related pathways for Mn oxidation. The results of our study deepen our understanding of the molecular mechanisms in the plant-endophyte symbiosis in biogeochemical Mn cycling.

Acknowledgements The authors thank Dr. Liang Zhang (Shandong Normal University) for the help of SEM-EDX data analyses; Dr. Xuejie Zhang (Shandong Normal University) for the suggestion of plant dissections; Mr. Liyan Wang (Shandong University) for TEM imaging of the strains.

Funding This work was supported by the National Natural Science Foundation of China (Grant No. 31640002), the Natural Science Foundation of Shandong Province (Grant No. ZR2015JL013), the China Postdoctoral Science Foundation (Grant No. 2016 M600551), and the International Postdoctoral Exchange Fellowship Program of China (Grant No. 20170058).

References

Adams LF, Ghiorse WC (1986) Physiology and ultrastructure of *Leptothrix discophora* SS-1. Arch Microbiol 145:126–135

Altschul SF, Gish W, Miller W, Myers EW, Lipman DJ (1990) Basic local alignment search tool. J Mol Biol 215:403–410

Andeer PF, Learman DR, Mcilvin M, Dunn JA, Hansel CM (2015) Extracellular haem peroxidases mediate Mn(II) oxidation in a marine *Roseobacter* bacterium via superoxide production. Environ Microbiol 17:3925–3936

Anderson CR, Johnson HA, Caputo N, Davis RE, Torpey JW, Tebo BM (2009) Mn(II) oxidation is catalyzed by heme peroxidases in "*Aurantimonas manganoxydans*" strain SI85-9A1 and *Erythrobacter* sp. strain SD-21. Appl Environ Microbiol 75:4130–4138

Andrades-Moreno L, Del Castillo I, Parra R, Doukkali B, Redondo-Gómez S, Pérez-Palacios P, Caviedes MA, Pajuelo E, Rodríguez-Llorente ID (2014) Prospecting metal-resistant plant-growth promoting rhizobacteria for rhizoremediation of metal contaminated estuaries using *Spartina densiflora*. Environ Sci Pollut Res Int 21:3713–3721

Benner SG, Blowes DW, Gould WD, Herbert RB, Ptacek CJ (1999) Geochemistry of a permeable reactive barrier for metals and acid mine drainage. Environ Sci Technol 33:2793–2799

Bohu T, Santelli CM, Akob DM, Neu TR, Ciobota V, Rösch P, Popp J, Nietzsche S, Küsel K (2015) Characterization of pH dependent Mn(II) oxidation strategies and formation of a bixbyite-like phase by *Mesorhizobium australicum* T-G1. Front Microbiol 6. https://doi.org/10.3389/fmicb.2015.00734

Brown JJ, Glenn EP, Fitzsimmons KM, Smith SE (1999) Halophytes for the treatment of saline aquaculture effluent. Aquaculture 175:255–268

Butterfield CN, Soldatova AV, Lee SW, Spiro TG, Tebo BM (2013) Mn(II,III) oxidation and MnO_2 mineralization by an expressed bacterial multicopper oxidase. Proc Natl Acad Sci U S A 110:11731–11735

Clement BG, Luther GW, Tebo BM (2009) Rapid, oxygen-dependent microbial Mn(II) oxidation kinetics at sub-micromolar oxygen concentrations in the Black Sea suboxic zone. Geochim Cosmochim Acta 73:1878–1889

Corstjens PLAM, De Vrind JPM, Goosen T, de Vrind-de Jong EW (1997) Identification and molecular analysis of the *Leptothrix discophora* SS-1 *mofA* gene, a gene putatively encoding a manganese-oxidizing protein with copper domains. Geomicrobiol J 14:91–108

Dick GJ, Torpey JW, Beveridge TJ, Tebo BM (2008) Direct identification of a bacterial manganese(II) oxidase, the multicopper oxidase MnxG, from spores of several different marine *Bacillus* species. Appl Environ Microbiol 74:1527–1534

El Gheriany IA, Bocioaga D, Hay AG, Ghiorse WC, Shuler ML, Lion LW (2009) Iron requirement for Mn(II) oxidation by *Leptothrix discophora* SS-1. Appl Environ Microbiol 75:1229–1235

Fernando DR, Lynch JP (2015) Manganese phytotoxicity: new light on an old problem. Ann Bot 116:313–319

Fernando DR, Mizuno T, Woodrow IE, Baker AJ, Collins RN (2010) Characterization of foliar manganese (Mn) in Mn (hyper)accumulators using X-ray absorption spectroscopy. New Phytol 188:1014–1027

Fernando DR, Marshall A, Baker AJ, Mizuno T (2013) Microbeam methodologies as powerful tools in manganese hyperaccumulation research: present status and future directions. Front Plant Sci 4(319). https://doi.org/10.3389/fpls.2013.00319

Geszvain K, McCarthy JK, Tebo BM (2013) Elimination of manganese(II,III) oxidation in *Pseudomonas putida* GB-1 by a double knockout of two putative multicopper oxidase genes. Appl Environ Microbiol 79:357–366

Godrant A, Rose AL, Sarthou G, Waite TD (2009) New method for the determination of extracellular production of superoxide by marine phytoplankton using the chemiluminescence probes MCLA and red-CLA. Limnol Oceanogr: Methods 7(10):682–692

Guo JR, Suo SS, Wang BS (2015) Sodium chloride improves seed vigour of the euhalophyte *Suaeda salsa*. Seed Sci Res 25:335–344

Guo JR, Li YD, Han GL, Song J, Wang BS (2018) NaCl markedly improved the reproductive capacity of the euhalophyte *Suaeda salsa*. Funct Plant Biol 45:350–361

Hansel CM, Zeiner CA, Santelli CM, Webb SM (2012) Mn(II) oxidation by an ascomycete fungus is linked to superoxide production during asexual reproduction. Proc Natl Acad Sci U S A 109:12621–12625

Hosseinkhani B, Emtiazi G (2011) Synthesis and characterization of a novel extracellular biogenic manganese oxide (bixbyite-like Mn_2O_3) nanoparticle by isolated *Acinetobacter* sp. Curr Microbiol 63:300–305

Jung WK, Schweisfurth R (1979) Manganese oxidation by an intracellular protein of a *Pseudomonas* species. Z Allg Mikrobiol 19:107–115

Khan N, Seshadri B, Bolan N, Saint CP, Kirkham MB, Chowdhury S, Yamaguchi N, Lee DY, Li G, Kunhikrishnan A, Qi F, Karunanithi R, Qiu R, Zhu YG, Syu CH (2016) Root iron plaque on wetland plants as a dynamic pool of nutrients and contaminants. Adv Agron 138:1–96

Kim OS, Cho YJ, Lee K, Yoon SH, Kim M, Na H, Park SC, Jeon YS, Lee JH, Yi H, Won S, Chun J (2012) Introducing EzTaxon-e: a prokaryotic 16S rRNA gene sequence database with phylotypes that represent uncultured species. Int J Syst Evol Microbiol 62:716–721

Kimura M (1980) A simple method for estimating evolutionary rates of base substitutions through comparative studies of nucleotide sequences. J Mol Evol 16:111–120

Krämer U (2010) Metal hyperaccumulation in plants. Annu Rev Plant Biol 61:517–534

Krumbein WE, Altmann HJ (1973) A new method for the detection and enumeration of manganese oxidizing and reducing microorganisms. Helgol wiss Meeresunters 25:347–356

Larkin MA, Blackshields G, Brown NP, Chenna R, McGettigan PA, McWilliam H, Valentin F, Wallace IM, Wilm A, Lopez R, Thompson JD, Gibson TJ, Higgins DG (2007) Clustal W and Clustal X version 2.0. Bioinformatics 23:2947–2948

Learman DR, Voelker BM, Vazquez-Rodriguez AI, Hansel CM (2011) Formation of manganese oxides by bacterially generated superoxide. Nat Geosci 4:95–98

Learman DR, Voelker BM, Madden AS, Hansel CM (2013) Constraints on superoxide mediated formation of manganese oxides. Front Microbiol 4. https://doi.org/10.3389/fmicb.2013.00262

Li X, Zhang XD, Song J, Fan H, Feng G, Wang BS (2011) Accumulation of ions during seed development under controlled saline conditions of two *Suaeda salsa* populations is related to their adaptation to saline environments. Plant Soil 341:99–107

Li X, Liu Y, Chen M, Song YP, Song J, Wang BS, Feng G (2012) Relationships between ion and chlorophyll accumulation in seeds and adaptation to saline environments in *Suaeda salsa* populations. Plant Biosyst 146:142–149

Liu QQ, Liu RR, Ma YC, Song J (2018) Physiological and molecular evidence for Na+ and cl- exclusion in the roots of two *Suaeda salsa* populations. Aquat Bot 146:1–7

Mendelssohn IA, Postek MT (1982) Elemental analysis of deposits on the roots of *Spartina alterniflora* Loisel. Am J Bot 69:904–912

Michalak I, Chojnacka K, Marycz K (2011) Using ICP-OES and SEM-EDX in biosorption studies. Microchim Acta 172:65–74

Minibayeva FV, Gordon LK, Kolesnikov OP, Chasov AV (2001) Role of extracellular peroxidase in the superoxide production by wheat root cells. Protoplasma 217:125–128

Miyata N, Tani Y, Maruo K, Tsuno H, Sakata M, Iwahori K (2006) Manganese (IV) oxide production by *Acremonium* sp. strain KR21-2 and extracellular Mn(II) oxidase activity. Appl Environ Microbiol 72:6467–6473

Pinto E, Sigaud-kutner TCS, Leitão MAS, Okamoto OK, Morse D, Colepicolo P (2003) Heavy metal-induced oxidative stress in algae. J Phycol 39:1008–1018

Saitou N, Nei M (1987) The neighbor-joining method: a new method for reconstructing phylogenetic trees. Mol Biol Evol 4:406–425

Soldatova AV, Butterfield C, Oyerinde OF, Tebo BM, Spiro TG (2012) Multicopper oxidase involvement in both Mn(II) and

Mn(III) oxidation during bacterial formation of MnO_2. J Biol Inorg Chem 17:1151–1158

Song J, Wang B (2015) Using euhalophytes to understand salt tolerance and to develop saline agriculture: *Suaeda salsa* as a promising model. Ann Bot 115:541–553

Spiro TG, Bargar JR, Sposito G, Tebo BM (2009) Bacteriogenic manganese oxides. Acc Chem Res 43:2–9

Su J, Bao P, Bai T, Deng L, Wu H, Liu F, He J (2013) CotA, a multicopper oxidase from *Bacillus pumilus* WH4, exhibits manganese-oxidase activity. PLoS One 8:e60573. https://doi.org/10.1371/journal.pone.0060573

Sui N, Tian SS, Wang WQ, Wang MJ, Fan H (2017) Overexpression of glycerol-3-phosphate acyltransferase from *Suaeda sals*a improves salt tolerance in *Arabidopsis*. Front Plant Sci 8. https://doi.org/10.3389/fpls.2017.01337

Sun WG, Gan ZT, Sun ZG, Li LL, Sun JK, Sun WL, Mou XJ, Wang LL (2013) Spatial distribution characteristics of Fe and Mn contents in the new-born coastal marshes in the Yellow River estuary. Huan Jing Ke Xue 34:4411–4419 In Chinese

Sundby B, Vale C, Cacador I, Catarino F (1998) Metal-rich concretions on the roots of salt marsh plants: mechanism and rate of formation. Limnol Oceanogr 43:245–252

Tamura K, Stecher G, Peterson D, Filipski A, Kumar S (2013) MEGA6: molecular evolutionary genetics analysis version 6.0. Mol Biol Evol 30:2725–2729

Tebo BM, Johnson HA, Mccarthy JK, Templeton AS (2005) Geomicrobiology of manganese (II) oxidation. Trends Microbiol 13:421–428

Tsuji K, Asayama T, Shiraki N, Inoue S, Okuda E, Hayashi C, Nishida K, Hasegawa H, Harada E (2017) Mn accumulation in a submerged plant *Egeria densa* (Hydrocharitaceae) is mediated by epiphytic bacteria. Plant Cell Environ 40: 1163–1173

Vale C, Catarino F, Cortesao C, Cacador M (1990) Presence of metal-rich rhizoconcretions on the roots of *Spartina maritima* from the salt marshes of the Tagus estuary, Portugal. Sci Total Environ 97/98:617–626

Vinogradov AD, Grivennikova VG (2005) Generation of superoxide-radical by the NADH: ubiquinone oxidoreductase of heart mitochondria. Biochemistry (Mosc) 70:120–127

Wang FX, Xu YG, Wang S, Shi WW, Liu R, Feng G, Song J (2015) Salinity affects production and salt tolerance of dimorphic seeds of *Suaeda salsa*. Plant Physiol Bioc 95:41–48

Wani ZA, Ashraf N, Mohiuddin T, Riyaz-Ul-Hassan S (2015) Plant-endophyte symbiosis, an ecological perspective. Appl Microbiol Biotechnol 99:2955–2965

Webb SM, Dick GJ, Bargar JR, Tebo BM (2005) Evidence for the presence of Mn(III) intermediates in the bacterial oxidation of Mn(II). Proc Natl Acad Sci U S A 102:5558–5563

Weis JS, Weis P (2004) Metal uptake, transport and release by wetland plants: implications for phytoremediation and restoration. Environ Int 30:685–700

Wu HF, Liu XL, Zhao JM, Yu JB (2012) Toxicological responses in halophyte *Suaeda salsa* to mercury under environmentally relevant salinity. Ecotoxic Environ Safe 85:64–71

Yamaji K, Nagata S, Haruma T, Ohnuki T, Kozaki T, Watanabe N, Nanba K (2016) Root endophytic bacteria of a 137Cs and Mn accumulator plant, *Eleutherococcus sciadophylloides*, increase 137Cs and Mn desorption in the soil. J Environ Radioactiv 153:112–119

Zhang WH, He LY, Wang Q, Sheng XF (2015a) Inoculation with endophytic *Bacillus megaterium* 1Y31 increases Mn accumulation and induces the growth and energy metabolism-related differentially-expressed proteome in Mn hyperaccumulator hybrid pennisetum. J Hazard Mater 30:513–521

Zhang WH, Chen W, He LY, Wang Q, Sheng XF (2015b) Characterization of Mn-resistant endophytic bacteria from Mn-hyperaccumulator *Phytolacca americana* and their impact on Mn accumulation of hybrid penisetum. Ecotoxic Environ Safe 120:369–376

Zhang Z, Lai J, Yin H, Feng X, Tan W, Liu F (2015c) Absorption mechanisms of Cu^{2+} on a biogenic bixbyite-like Mn_2O_3 produced by *Bacillus* CUA isolated from soil. Geochem T 16(5):5. https://doi.org/10.1186/s12932-015-0020-6

Zhang Z, Zhang Z, Chen H, Liu J, Liu C, Ni H, Zhao C, Ali M, Liu F, Li L (2015d) Surface Mn(II) oxidation actuated by a multicopper oxidase in a soil bacterium leads to the formation of manganese oxide minerals. Sci Rep 5(10895). https://doi.org/10.1038/srep10895

Zhou JC, Fu TT, Sui N, Guo JR, Feng G, Fan JL, Song J (2016) The role of salinity in seed maturation of the euhalophyte *Suaeda salsa*. Plant Biosyst 150:83–90